

Advances in Materials Used in Civil and Construction Engineering

Advances in Materials Used in Civil and Construction Engineering

Edited by

Syed Ali Rizwan, Shahid Ali,
Muzna Anam and Bilal Zahid

**Cambridge
Scholars
Publishing**



Advances in Materials Used in Civil and Construction Engineering

Edited by Syed Ali Rizwan, Shahid Ali, Muzna Anam and Bilal Zahid

This book first published 2025

Cambridge Scholars Publishing

Lady Stephenson Library, Newcastle upon Tyne, NE6 2PA, UK

British Library Cataloguing in Publication Data

A catalogue record for this book is available from the British Library

Copyright © 2025 by Syed Ali Rizwan, Shahid Ali, Muzna Anam,
Bilal Zahid and contributors

All rights for this book reserved. No part of this book may be reproduced, stored in a retrieval system, or transmitted, in any form or by any means, electronic, mechanical, photocopying, recording or otherwise, without the prior permission of the copyright owner.

ISBN: 978-1-0364-4963-6

ISBN (Ebook): 1-0364-4963-7

TABLE OF CONTENT

LIST OF ILLUSTRATIONS	ix
LIST OF TABLES.....	xviii
FOREWORD	xxi
PREFACE	xxii
ACKNOWLEDGMENTS	xxiii
LIST OF ABBREVIATIONS	xxiv
CIVIL ENGINEERING MATERIALS.....	1
CHAPTER ONE.....	2
<i>Development of Geopolymer Mortar at Ambient Condition by Using Limestone powder</i>	<i>2</i>
CHAPTER TWO	13
<i>Measurement of Temperature Distribution in Freezing/Thawing concrete</i>	<i>13</i>
CHAPTER THREE	22
<i>Systematic Approach to Develop Geopolymer Brick by Single, Binary and Ternary Binders.....</i>	<i>22</i>
CHAPTER FOUR	33
<i>Characterization of Novel Alkaliphilic Calcifying Bacteria for Sustainable Bio-Based Concrete Self-Healing Mechanism.....</i>	<i>33</i>
CHAPTER FIVE	56
<i>Strength Enhancement of Rubberized Concrete by Using Chemically Treated Rubber Particles as Partial Replacement of Sand.....</i>	<i>56</i>

CHAPTER SIX.....	72
<i>EVALUATION OF PHYSICAL & MECHANICAL PROPERTIES OF STEEL FIBER</i>	
<i>REINFORCED CONCRETE</i>	72
CHAPTER SEVEN	88
<i>Sustainable Performance of Geopolymer Mortars as Modern</i>	
<i>Concrete Surface Repair Materials</i>	88
CHAPTER EIGHT.....	100
<i>Developing Self-Healing and Self-Sensing Multipurpose Smart Mortar</i>	
<i>Modified with Graphitic Insertions</i>	100
CHAPTER NINE.....	121
<i>Performance Evaluation of Powder Reactive Concrete Using a</i>	
<i>Composite Mixture of Ceramic and Brick Powders as Partial</i>	
<i>Replacement of Cement.....</i>	121
CHAPTER TEN	134
<i>Early-age Linear Shrinkage of Self Compacting Mortar Systems</i>	
<i>(SCMs) Containing Super Absorbent Polymers (SAPs)</i>	134
CHAPTER ELEVEN.....	156
<i>Effect of Size of TiO₂ Nano-Particles on Physical and Mechanical</i>	
<i>Properties of Self-Compacting Cement Paste Systems</i>	156
CHAPTER TWELVE	177
<i>Development of Sustainable Construction Materials and Products</i>	
<i>Using Multiscale Investigation Approach</i>	177
CHAPTER THIRTEEN.....	198
<i>Effective Micro-organisms and Wood Saw Dust Enhance Response of</i>	
<i>Eco-Friendly Self-Consolidating Paste Systems.....</i>	198
CHAPTER FOURTEEN.....	233
<i>Effect of Methylcellulose on the Strength Properties of Concrete ..</i>	233
STRUCTURAL ENGINEERING	255
CHAPTER FIFTEEN	256
<i>EXPLORING DESIGN EFFICIENCY USING BIM FOR APPLICATION IN</i>	
<i>PAKISTAN</i>	256
CHAPTER SIXTEEN	279
<i>Structural Performance of Building Façade for Sustainable Design</i>	279

CHAPTER SEVENTEEN	292
<i>Circular Economy Implications for Construction and Demolition</i>	
<i>Waste in Pakistan</i>	292
CHAPTER EIGHTEEN	311
<i>Study On Sustainable Construction in Pakistan by Use Of Fly Ash</i>	
<i>Bricks.....</i>	311
CHAPTER NINETEEN	323
<i>Finite element analysis of GFRP-Reinforced Geopolymer Concrete</i>	
<i>Circular Columns under Concentric Loading</i>	323
WATER RESOURCES AND ENVIRONMENTAL ENGINEERING	341
CHAPTER TWENTY	342
<i>Recycling industrial wastes in manufacturing of concrete and bricks:</i>	
<i>From waste to wealth.....</i>	342
CHAPTER TWENTY-ONE	357
<i>Climate change and variability in Pakistan: A case study of Swat River</i>	
.....	357
CHAPTER TWENTY-TWO	381
<i>Performance comparison of complete mix reactor and monolithic</i>	
<i>static mixer in Ballasted Flocculation</i>	381
CHAPTER TWENTY-THREE	400
<i>Assessment of streamflows at Haro River Basin using Climate</i>	
<i>Forecast System Reanalysis Dataset in Soil and Water Assessment</i>	
<i>Tool.....</i>	400
CHAPTER TWENTY-FOUR	410
<i>Experimental Study of Potential Use of Treated Wastewater on</i>	
<i>Compaction and Shear Strength of Silty Sand</i>	410
CHAPTER TWENTY-FIVE	419
<i>Development of Regional IDF Relationships for Oman.....</i>	419
CHAPTER TWENTY-SIX	437
<i>Performance Evaluation and Bias Adjustment of GSMaP Rainfall</i>	
<i>Estimates for Ravi River Basin, Pakistan.....</i>	437

CONSTRUCTION MANAGEMENT 461

CHAPTER TWENTY-SEVEN 462

Advanced Digitalization Technologies for Design, Construction, and Building Operations: Impact, Challenges, and the Path Forward... 462

CHAPTER TWENTY-EIGHT 479

Performance-based design for structures: The need and the process..... 479

CHAPTER TWENTY-NINE 495

Minimizing Clash-Related Delays in Building Construction by Adopting Building Information Modeling..... 495

CHAPTER THIRTY 509

Standardizing Qualifications and Mobilizing Engineering Professionals for 2030 Agenda for Sustainable Development..... 509

LIST OF CONTRIBUTORS..... 511

LIST OF ILLUSTRATIONS

Fig. 1-1: Schematic Diagram of Specimen Preparation.....	6
Fig. 1-2: Influence of Curing Condition on the Compressive Strength of Fa-Lime Geopolymer Mortar	7
Fig. 1-3: Influence Of A/P Ratio.	8
Fig. 1-4: Influence Of Type Of Sand.....	9
Fig. 1-5: Bulk Density And Compressive Strength of All Types of Specimens.....	10
Fig. 2-1: (Left) optical fiber sensor housing glued on concrete surface. (right) T-type thermocouple cast in mortar specimen.....	17
Fig. 2-2: Temperature development obtained at 5mm below the test surface by optical fiber sensor at the edge (Left) and by cast-in thermocouple at the central axis (right)	19
Fig. 3-1: Particle size distribution of FA and BA	26
Fig. 3-2: Particle size distribution of DS	26
Fig. 3-3: Influence of moulding pressure on compressive strength of FA-based geopolymer paste	28
Fig. 3-4: Compressive strength of geopolymer paste with binary precursors FA, and BA	29
Fig. 3-5: Compressive strength of geopolymer pate (binary precursors: FA, and DA; ternary precursors: FA, BA, and DS).....	30
Fig. 4-1: (a) Screening of calcifying bacteria through CPM Plate (b) 15ml 0Falcon tube depicting white precipitate at the bottom	41
Fig. 4-2: Bacterial calcite quantification for calcium lactate and calcium acetate	42
Fig. 4-3: Isolated bacterial calcite qualification at pH7 pH10	43
Fig. 4-4: Spore former (left), Non-spore former(right).....	43
Fig. 4-5: Gram-positive bacilli and cocci bacteria.....	44
Fig. 4-6: Oxidase-positive and negative strains output.....	44
Fig. 4-7: Catalyze negative and positive strains output	44
Fig. 4-8: Phylogenetic tree based on the bacterial 16S rRNA gene sequence data of different isolates available in the GenBank database	48

Fig. 4-9: Effect of calcium source on calcite morphology; (A) calcite precipitates of calcium locate sources are mostly spherical vaterite (A.1) and rhombohedral calcite crystals (A.2). (B) calcite precipitates of calcium acetate source are mainly spherical oval vaterite (B.2) few are rhombohedral (B.1) and amorphous CaCO_3 (B.3)	49
Fig. 4-10: XRD patterns of precipitated calcite	50
Fig. 4-11: TG curve of precipitated calcite	51
Fig. 5-1: Concrete ingredients (a) fly ash, (b) silica fumes, (c) Waste Crumb Rubber, (d) Sand, (e) Coarse aggregates, and (f) NaOH	63
Fig. 5-2: Specimen preparation (a) Mixing (b) Casting, and (c) Curing...	63
Fig. 5-3: Slump Test	64
Fig. 5-4: Graphical representation of results of slump test	65
Fig. 5-5: Graphical representation of results of density test	66
Fig. 5-6: Graphical representation of compressive strength test results ...	67
Fig. 5-7: Graphical representation of flexural strength tests	68
Fig. 5-8: Graphical representation of splitting tensile strength test	68
Fig. 6-1: Gradation curve for fine aggregate	76
Fig. 6-2: Crumpled shape	77
Fig. 6-3: Mixing of Control Concrete	78
Fig. 6-4: Mixing of steel fiber	79
Fig. 6-5: Comparison of compressive strength of steel fiber reinforced concrete	83
Fig. 6-6: Comparison of split tensile strength of SFRC & CC	84
Fig. 6-7: Comparison of flexural strength of steel fiber reinforced concrete	85
Fig. 7-1: Geometry of slant share bond strength test	93
Fig. 7-2: Strength development of ternary blended GPMs	95
Fig. 7-3: Effects of various WCT: GBFS: FA ratios on the XRD patterns of GPMs	96
Fig. 7-4: Effects of various WCT: GBFS: FA ratios on SSBS of GPMs at 28 days of age	97
Fig. 8-1: Piezoresistive testing	107
Fig. 8-2: Compressive strength of smart mortar at increasing curing periods	108
Fig. 8-3: Compressive strength recovered for pre-cracked specimens after healing under, (a) 28 days wet curing, (b) 56 days wet curing	111

Fig. 8-4: Resistivity of graphitic formulations against varying loading conditions. (a) no load, (b) ultimate compressive load, (c) cyclic compressive load	113-114
Fig. 9-1: (a) Ceramic waste, (b) Waste bricks in landfills	123
Fig. 9-2: Powder form (a) waste ceramic, (b) waste brick.....	125
Fig. 9-3: XRD images of WCP and WBP	126
Fig. 9-4: Strength activity index for (a) waste brick powder, (b) waste ceramic powder.....	128
Fig. 9-5: Workability as a function of combined WCP and WBP content..	128
Fig. 9-6: (a) Compressive, (b) tensile, and (c) flexural strengths as a function of waste	129
Fig. 10-1: Scanning electron micrograph of an individual SAP particle ..	138
Fig. 10-2: Chemical Composition of SAP	138
Fig. 10-3: Method of Graduated Cylinders.....	142
Fig. 10-4: Modified German shrinkage channel apparatus used to measure linear shrinkage of SCM systems	145
Fig. 10-5: Shrinkage in SCM systems with 0.38 w/c (basic) at different amounts of SAP	146
Fig. 10-6: Shrinkage in SCM systems with 0.4 w/c (basic) at different amounts of SAP	146
Fig. 10-7: Shrinkage of SCM systems with 0.42 W/C (basic) at different amounts of SAP	147
Fig. 10-8: Flow of SCM formulations	148
Fig. 10-9: Flow times of SCM formulations.....	148
Fig. 10-10: Compressive strength of SCM formulations at 1,3 and 28 days.....	149
Fig. 10-11: Flexural Strength of SCM formulations for 1,3 and 28 days.....	149
Fig. 11-1: Different forms of TiO ₂	158
Fig. 11-2: SEM of TiO ₂ nanoparticles; (a) 20nm Anatase; (b) 15nm Anatase (c) 5nm Amorphous + Anatase	162
Fig. 11-3: Mechanically operated Hagerman's Cone apparatus.....	164
Fig. 11-4: SCP with 30cm flow	165
Fig. 11-5: Superplasticizer demand	166
Fig. 11-6: Flexural strength of SCP systems having Titania particles....	167
Fig. 11-7: XRD diffractograms for formulations with 5nm particle sizes @ 1 Day.....	168

Fig. 11-8: XRD/DTG/TGA Diffractograms for formulations with 5nm particle sizes @ 1Day	168
Fig. 11-9: Heat flow of SCP with N30 Particles.....	169
Fig. 11-10: Heat flow of SCP with N15 Particles.....	169
Fig. 11-11: Heat flow of SCP with N5 Particles.....	170
Fig. 11-12: Heat flow of SCP with CEM I and 1% replacement.....	170
Fig. 11-13: MIP Results of N5-1.00 at 3 Ages	171
Fig. 11-14: MIP Results of CEM I and N5-1.00 at 3 days	172
Fig. 11-15: MIP Results of CEM I and N5-1.00 at 7 days	172
Fig. 12-1: At multi-scale module showing different scales of paste.....	181
Fig. 12-2: Self-curing of samples using polythene sheet.....	183
Fig. 12-3: Cylindrical specimen of 75mm diameter and 225mm length ..	183
Fig. 12-4: Bagasse ash	185
Fig. 12-5: Short-term creep test of cement paste	185
Fig. 12-6: (a) Mold for cylindrical specimens (b) Brick manufacturing machine (c) Brick specimens.....	187
Fig. 12-7: Compressive strength of the pastes and mortars at different ages	188
Fig. 12-8: a, b, c, d, e & f (Creep strain parameter's graphical relation of cement paste).....	189
Fig. 12-9: Creep Function [10^{-6} / MPa] VS time relation for cement paste.....	190
Fig. 12-10: a, b, c, d, e (Creep strain parameter's graphical relation of cement mortar).....	191
Fig. 12-11: Creep function [10^{-6} / MPa] VS time relation for cement mortar	191
Fig. 12-12: a, b, c, d, e (creep strain parameter's graphical relation of bagasse cement paste).....	192
Fig. 12-13: Creep function [10^{-6} / MPa] Vs time relation for bagasse ash paste.....	193
Fig. 12-14: a, b, c, d, e, & f (creep strain parameter's graphical relation of bagasse ash mortar)	194
Fig. 12-15: Creep Function [10^{-6} / MPa] VS time relation for bagasse ash mortar	195
Fig. 13-1: (a) Deodar Soft Wood SD (SWSD) (b) Sheesham Hard Wood SD (HWSD).....	204
Fig. 13-2: Particle size distribution (grading) curves for Soft Wood (Deodar) & Hard Wood (Sheesham) sae dust.....	205

Fig. 13-3: SEM Image of Deodar @200 micro meter	206
Fig. 13-4: SEM Image of Sheesham @200 micro meter	206
Fig. 13-5: FTIR Spectrograph of a) Sheesham b) Deodar	209
Fig. 13-6: Early Shrinkage Apparatus	213
Fig. 13-7: F-CAL Calorimetry.....	213
Fig. 13-8: Initial and final setting time for cement paste4 specimens	215
Fig. 13-9: Super plasticizer demand for SCP's formulation.....	215
Fig. 13-10: Water Demand for SCP Formulation.....	216
Fig. 13-11: Air Content of SCP's	219
Fig. 13-12: Densities for SCP's	220
Fig. 13-13: Calorimetric Curves for SWSD SCPs Formulations.....	220
Fig. 13-14: Early age shrinkage strain of SCP systems	221
Fig. 13-15: Compressive strength of SCP formulations at different ages.....	221
Fig. 13-16: XRD Pattern of SCPs containing 2% unfermented SD, Control Sample, and 2% Fermented SD.....	222
Fig. 13-17: SEM Micrographs of (a) Control Formulation, (b) 2% Unfermented Sawdust Deodar, and (c) 2% Fermented Sawdust Deodar	224-225
Fig. 14-1: Casted concrete and mortar samples	237
Fig. 14-2: Gradation curve of Lawrencepur sand	239
Fig. 14-3: Gradation curve of Margalla Crush	240
Fig. 14-4: Concrete Tensile Strength.....	241
Fig. 14-5: SEM for methyl cellulose	243
Fig. 14-6: Concrete Compressive Strength.....	244
Fig. 14-7: Compressive strength of concrete cube specimens	245
Fig. 14-8: Rate of gain of strengths, concrete cubes.....	245
Fig. 14-9: Effect of methylcellulose on ratio of cube to cylinder compressive strength	247
Fig. 14-10: Increase in compressive strength of cement mortar cubes and concrete cubes.....	248
Fig. 14-11: Modulus of Rupture Test	250
Fig. 14-12: Effect of Methylcellulose on Modulus of Rupture of Concrete.....	251
Fig. 15-1: AutoCAD plan view 1	266
Fig. 15-2: AutoCAD plan view 2	266
Fig. 15-3: Color Scheme of 1 st Floor	267
Fig. 15-4: Color Scheme of 2 nd Floor	267

Fig. 15-5: Revit 3D model.....	267
Fig. 15-6: 3D cut view	267
Fig. 15-7: Frame structure	268
Fig. 15-8: RSA analysis.....	268
Fig. 15-9: Beam drawing	269
Fig. 15-10: Column drawings	270
Fig. 15-11: Slab drawing	271
Fig. 15-12: Clash Case 1.....	272
Fig. 15-13: Clash Case 2.....	272
Fig. 16-1: Grenfell tower-before (a) and after reinforcement (b)	281
Fig. 16-2: Inferno timeline for Grenfell Tower	282
Fig. 16-3: a) the building façade and fire breakout; b) Details of the façade.....	282
Fig. 16-4: Wave effect in Aquatic Center Façade in Melbourne Australia	285
Fig. 16-5: Earth and Cloud effect in Parking Lot in Sydney Australia...	285
Fig. 16-6: Ventilation Chamber on the roof using perforated metal sheets as façade, acting as both a barrier (against potentially small animals such as birds) and allowing free air to flow out.....	286
Fig. 16-7: Cable Truss Façade for Hospital Building	286
Fig. 16-8: Aesthetical pleasing and sustainable Façade improves precinct value	287
Fig. 16-9: Provision of Sunshades & Fall Protection in school building ..	288
Fig. 16-10: Quality control by site checks to ensure Sustainability.....	289
Fig. 17-1: An investigation framework for C&D waste minimisations....	294
Fig. 18-1: Bricks in water tray during (a) Fly ash (b) Clay	315
Fig. 18-2: Plan of 62' x 72' Apartment	316
Fig. 18-3: Cost of foundation brickwork	319
Fig. 18-4: Water absorption of brick sample	319
Fig. 18-5: Cost of super-structure brickwork.....	320
Fig. 18-6: total cost of brickwork	320
Fig. 19-1: Geometry of specimen in mm units	327
Fig. 19-2: Tensile behavior of reinforcement bars R8, N10, G8 and G10	329
Fig. 19-3: Stress-strain behavior of 50MPa GPC	329
Fig. 19-4: Simulated FEM.....	330

Fig. 19-5: Comparison between the failure modes of steel40, GFRP40, and GFRP75, respectively obtained from experiments & FEM models	333
Fig. 19-6: Comparison between experimental and FEM load-deformation curve of STEEL40	334
Fig. 19-7: Comparison between experimental and FEM load-deformation curve of GFRP40	334
Fig. 19-8: Comparison between experimental and FEM load-deformation curve of GFRP75	335
Fig. 19-9: Comparison between experimental and FEM results with mesh size 100 and 75	336
Fig. 19-10: Load deformation curve of different pitch sizes	337
Fig. 19-11: Load deformation curve column with concrete grade 50MPa and 55 MPa.....	338
Fig. 20-1: Aggregates (a) sand, (b) coarse (5mm-10mm), (c) Aggregate 20mm.....	348
Fig. 20-2: Industrial waste slag (a) raw form, (b) powder form	349
Fig. 20-3: Strength test (a) compressive, (b) tensile and (c) flexural.....	352
Fig. 20-4: Compressive strength.....	353
Fig. 20-5: Split cylinder tensile strength at 28 days.....	353
Fig. 20-6: Flexural strength	354
Fig. 21-1: Location map of Swat river basin	360
Fig. 21-2: Percentage correlation of ENSO cycle and precipitation in Jul-Aug-Sep from 1948-2010	361
Fig. 21-3: Projected average changes in Tmax and Tmin concerning the baseline period 1979-2014 under RCPs 4.5 and RCP 8.5 in Swat river basin	362-363
Fig. 21-4: Projected absolute annual Tmax under RCP 4.5 and RCP 8.5 for 2020, 2050s and 2080s in Swat River basin.....	364-365
Fig. 21-5: Projected absolute annual average Tmin under RCP 4.5 and RCP 8.5 in Swat river basin.....	366-369
Fig. 21-6: Projected average annual percentage changes in precipitation with respect to the baseline period 1979-2014 under RCPs 4.5 & 8.5 in Swat river basin	370
Fig. 21-7: Projected average seasonal precipitation of Swat river basin under RCP 4.5(a) and RCP 8.5(b) by three RCMs.....	376-377

Fig. 21-8: Projected average seasonal changes in precipitation (%) with respect to baseline period (1979-2014) in the Swat river basin under RCP 4.5(a) and RCP 8.5(b), by three RCMs'	378-379
Fig. 22-1: Characteristics of ballast adopted in this study	385
Fig. 22-2: Callibration of Jar test operation.....	386
Fig. 22-3: Timeline of Static mixer and jar test operations leading to the floc characterization using image analysis	389
Fig. 22-4: Initial pH optimization at applied coagulant concentration (PACI: 30mgL ⁻¹).....	390
Fig. 22-5: Determination of clarification(%) of highly turbid influent...	392
Fig. 23-1: Location of study area.....	403
Fig. 23-2: Watershed Delineation in SWAT	406
Fig. 23-3: Yearly flow simulated in seventeen Sub-basins.....	407
Fig. 24-1: Proctor testing	414
Fig. 24-2: Soil samples	414
Fig. 24-3: Comparison between dry density and moisture content of TW and TWW	415
Fig. 24-4: Comparison of normal and shear strength of TW and TWW at 0,41 and 120 days	416
Fig. 24-4: Graph b/w degree of saturation and shear strength of TW and TWW at 10kPa at 0.41 and 120 days.....	416
Fig. 25-1: Map of Sultanate of Oman	422
Fig. 25-2: Methodology for developing IDF relationship	428
Fig. 25-3: IDF Curves for Mazara station.....	430
Fig. 25-4: Contours of e curve in IDF relationship.....	433
Fig. 25-5: Contours of m value in IDF relationship.....	434
Fig. 25-6: Contours of C value in IDF relationship.....	434
Fig. 26-1: Study region with the positions of rain stations outlined through SRTM 30-meter DEM.....	443
Fig. 26-2: Comparison of scatter plots for daily point rainfall of the study region for years 2014-2016.....	450
Fig. 26-3: Mean annual guage-based and GSMaP-based rainfalls	451
Fig. 26-4: Comparison of scatter plots for average rainfall of the study region for years 2014-2016.....	452
Fig. 26-5: Flow hydrographs generated for gauge, GSMaP and adjusted GSMaP estimates by HEC-HMS model for years 2014-2016.....	455
Fig. 26-6: Comparison for flows generated by HEC-HMSmodel for years 2014-2016.....	456

Fig. 27-1: Construction 4.0 technologies and their applications in the project life cycle	466
Fig. 28-1: Various performance levels in PBD.....	481
Fig. 28-2: Linking the damage to various performance levels in PBD...	481
Fig. 28-3: Various types of hazards that can affect structural safety and lead to disasters.....	482
Fig. 28-4: Constituents of disaster	483
Fig. 28-5: The responsibility for safety in the modern days can be spread among many stakeholders.....	484
Fig. 28-6: Typical building code	489
Fig. 28-7: Earthquake hazard level.....	490
Fig. 28-8: Schematic diagram showing the methodology for PBD	491
Fig. 28-9: Linking hazards to design decisions	491
Fig. 29-1: Ducts VS wall (before resolving).....	500
Fig. 29-2: Ducts VS Walls (After resolving).....	500
Fig. 29-3: Clashes percentage chart.....	501
Fig. 29-4: Number of clashes with resolving time.....	503

LIST OF TABLES

Table 1-1: Summary of mix proportion and the specimens prepared in all series	6
Table 2-1: Analysis of temperature sensors according to set standards....	15
Table 3-1: The XRF analysis of FA, BA, and DS (main oxides)	25
Table 3-2: Physical properties of DS.....	25
Table 4-1: Physical and chemical properties of selected soil samples.....	40
Table 4-2: Properties of selected isolated strains.....	46-47
Table 5-1: Physical properties of Fly ash and silica fumes.....	60
Table 5-2: Physical properties of crumb rubber	60
Table 5-3: Physical properties of cement	61
Table 5-4: Physical properties of sand.....	61
Table 5-5: Physical properties of Coarse aggregate	62
Table 6-1: Properties of cement.....	75
Table 6-2: Properties of Fine Aggregates	75-76
Table 6-3: Properties of Coarse Aggregates	76-77
Table 6-4: Mix Design.....	78
Table 6-5: Compressive strength results of control concrete.....	80
Table 6-6: Split tensile strength results of control concrete.....	81
Table 6-7: Flexural Tensile strength results of control concrete	81
Table 6-8: Compressive strength values of steel fiber reinforced concrete.....	82
Table 6-9: Split tensile strength values of steel fiber reinforced concrete.....	82
Table 6-10: Split tensile strength values of steel fiber reinforced concrete.....	83
Table 7-1: Mixture design of ternary blended (WCT, GBFS and FA) geopolymers	92
Table 8-1: Mix proportions of different formulations	105
Table 8-2: Cycle durations for cyclic compressive loading.....	106
Table 8-3: Average healed crack-widths across all curing ages of each formulation and overall average of crack-width healed.....	109
Table 9-1: Physical properties of cement, fine and coarse aggregates ...	125
Table 9-2: Chemical composition of cement, WCP and WBP	126

Table 9-3: Elemental composition in concrete specimen as a function of waste content	127
Table 10-1: Chemical characterization of cement	138-139
Table 10-2: SCM formulations and their compositions.....	140
Table 10-3: Dry density of SAP using Volume displacement method ...	143
Table 10-4: Absorption Capacity of SAP-Sieve Method.....	144
Table 10-5: Absorption Capacity of SAP-Graduated Cylinder Method...	144
Table 11-1: XRF of cement.....	160
Table 11-2: Physical properties of CEM I.....	160
Table 11-3: Physical properties of TiO ₂ nanoparticles	161
Table 11-4: Chemical composition of TiO ₂	161
Table 11-5: Test Formulations	163
Table 11-6: Average pore size of different formulations.....	173
Table 12-1: Mix proportion of controlled samples and SCMs samples....	182
Table 12-2: Chemical composition of materials.....	184
Table 12-3: Physical properties of OPC cement BA	184
Table 12-4: Properties of fine aggregates	184
Table 13-1: Chemical and physical analysis of OPC.....	203
Table 13-2: Characteristics of EMD.....	207
Table 13-3: Water absorption capacity of saw dust by using tea bag method	208
Table 13-4: Self compacting paste system formulations	211
Table 13-5: Thermal conductivity of SCP formulations.....	223
Table 14-1: Types of Specimens and their designations	237
Table 14-2: Physical properties of cement	238
Table 14-3: Tensile strength of concrete with methylcellulose	242
Table 14-4: Compressive strength of concrete cylinders with methylcellulose	244
Table 14-5: Mortar cubes compressive strength.....	249
Table 15-1: Global adoption rates	258
Table 15-2: Barriers to implementation of BIM.....	261-263
Table 17-1: A matrix summarizing the issues, strategies and stakeholders across the different stages of LoWMoR	306
Table 18-1: Details of samples	314
Table 19-1: Compressive and tensile properties of reinforcement	328
Table 19-2: Experimental and FEM results of Steel40, GFRP40, GFRP75 with respect to peak deflection and peak load	332
Table 20-1: Properties of cement.....	347

Table 20-2: Chemical properties of OPC	348
Table 20-3: Physical properties of aggregates	349
Table 20-4: Concrete composition.....	351
Table 21-1: Seasonal average future temperature (degree celcius) in Swat river basin with three RCMs under RCP 4.5	372
Table 21-2: Seasonal average future temperature (degree celcius) in Swat river basin with three RCMs under RCP 8.5	373
Table 21-3: Average increase in temperature (degree celcius) baseline period:1979-2014) in Swat river basin with three RCMs under RCP4.5	374
Table 21-4: Average increase in temperature (degree celcius) baseline period:1979-2014) in Swat river basin with three RCMs under RCP8.5	375
Table 22-1: Experimental conditions applied to Jar test and static mixer operation	388
Table 22-2: Control Experiment conditions	391
Table 24-1: Results of water sample	414
Table 24-2: Sieve analysis result	415
Table 25-1: The intensity, duration and return period of rainfall at Mazara station, Muscat.....	429
Table 25-2: Parameters of IDF relationship for all the stations	430-432
Table 26-1: Behavior of various SPEs over different study areas	441
Table 26-2: Basic information about GSMaP estimates.....	444
Table 26-3: Statistical parameters used in the comparison and evaluation	445
Table 26-4: Primary and secondary statistical indices before the execution of bias ammendment.....	453
Table 26-5: Primaery statistical indices later the execution of bias ammendment	453
Table 28-1: Acceptance criteria.....	488
Table 29-1: Clashed resolving time.....	502

FOREWORD

It gives me great pleasure to introduce the proceedings of the conference organized by the National University of Computer and Emerging Sciences (FAST) titled "Advances in Civil and Construction Engineering" held in December 2022. These proceedings present a remarkable collection of research papers presented and discussions held during the conference.

In these proceedings, readers will find a wealth of knowledge and innovation in the form of cutting-edge research papers, enlightening case studies, and thought-provoking discussions. The diverse range of topics covered in the conference represents the dynamic nature of civil and construction engineering, including but not limited to structural analysis and design, sustainable infrastructure development, construction materials and techniques, project management, and emerging technologies. The technical contributions from esteemed professionals, researchers, and participants from academia from around the globe, highlight the ongoing efforts to address the challenges in our ever-evolving built environment.

It is my sincere hope that these proceedings will serve as a valuable information source for the international community of civil and construction engineers, consultants, policymakers, and other stakeholders. I believe that the collective wisdom contained within this compilation will inspire further innovation and foster collaboration for advancement in civil engineering.

I extend my heartiest gratitude and appreciation to all the authors, reviewers, organizers, and conference participants who made this publication possible.

Dr. Tahir Masood
Managing Director and President
National Engineering Services Pakistan Pvt. Ltd.

Lahore Pakistan
December 2022

PREFACE

This book is a collection of the proceedings of an international conference called the International Conference on “**Advances in Civil and Construction Engineering ACCE 2022**”, held from December 1st-3rd, 2022, at the University of Management and Technology and the National University of Computer and Emerging Sciences in Lahore. The papers were invited on almost all aspects of these two engineering specialties and were subjected to a two-stage peer review. The percentage of selected papers was around 25%. The book contains several chapters, such as civil engineering materials, structural engineering, water resources and environmental engineering, construction management, and transportation engineering. The presented papers have been grouped under the aforementioned areas. It is worth noting that approximately 90 percent of the speakers were world-class researchers and academicians, while the remaining 10 percent represented top-tier universities from Pakistan. The book presents the latest and state-of-the-art papers that are essential for leading consultants, academicians, and contractors. It is hoped that the readers will find this book as a valuable collection of their liabilities. In case of further information, the undermentioned may kindly be contacted.

Prof. Dr Syed Ali Rizwan
Civil Engineering Department, Fast
Lahore, Pakistan

ACKNOWLEDGMENTS

On behalf of **Rector NUCES-FAST Dr. Aftab Maroof** and **Air Marshal Asif Raza**, Rector University of Management and Technology, the undermentioned is deeply indebted to them for their wholehearted support, encouragement,, and patronage.

I am also grateful to the technical committees, review experts, organizing committees, and management committees for their untiring support. Thanks, are also due to representors who came from around the globe to present their work and interact with their Pakistani counterparts. I would also like to extend my vote of thanks to **Muhammad Bilal Zahid (UMT)**, **Engr. Waqas Ajmal**, **Engr. Muzna Anam**, **Engr. Abdul Moeiz Khan**, **Engr. Muhammad Tayyab** and **Engr. Abdul Rafey Asad (NUCES-FAST)** for their help. Without their help, it would have been an impossible task.

A special thanks goes out to the book editors, **Engr. Abdur Rehman Zahid (NUCES-FAST)** and **Engr. Noor Fatima (NUCES-FAST)**, for their invaluable work and the indelible mark they leave on every page.

LIST OF ABBREVIATIONS

a, b = empirical constants in IDF relationships

C = empirical constant in IDF relationship

d = rainfall duration (T)

e = empirical constant in IDF relationship

i = rainfall intensity (L/T)

K = empirical function in IDF relationship

K_T = Frequency factor

m = empirical constant in IDF relationship

P = Precipitation (rainfall) (L)

T_r = Return period (years)

S = Standard deviation

x = Observed value

\bar{X} = Mean of observed values

CIVIL ENGINEERING MATERIALS

CHAPTER ONE

DEVELOPMENT OF GEOPOLYMER MORTAR AT AMBIENT CONDITION BY USING LIMESTONE POWDER

KHURAM RASHID AND KHADIJA MAWRA

Biographies

Khuram RASHID is an Associate Professor at the University of Engineering and Technology, Lahore, Pakistan. He received his Bachelor's and Master's from the same university and PhD from Japan. He is a member of the Pakistan Engineering Council, and Pakistan Engineering Congress, and was a member of the Asian Concrete Federation, and Japan Concrete Institute. His research interests include the development and performance of sustainable construction materials and strengthening of reinforced concrete structures.

Khadija MAWRA is a lecturer at the University of Engineering and Technology, Lahore, Pakistan. She completed her Master's degree in Construction Engineering and Management from NUST, Pakistan. Her research interests are Sustainability, Modular Construction, and Building Information Modelling.

Abstract

Geopolymer is an emerging material in the construction industry, but hot curing is required for the strength evolution of low calcium fly ash (FA) based geopolymer, which makes it energy intensive and is not suitable for real application. Although slag was added to attain strength at ambient conditions, but it increases the cost, and its availability is also an issue. Therefore, this work was designed, to get the strength at ambient conditions

by activating widely available uncalcined lime powder and FA in the alkaline environment (a combination of NaOH and Na_2SiO_3). River sand was also incorporated to develop geopolymer mortar. Specimens were exposed to three curing regimes; ambient curing, sun-dried, and hot curing and finally compressive strength was evaluated after 7 days. It was observed that due to the addition of limestone powder(LSP), the strength at ambient conditions was 26 MPa, and it further increased (39 MPa) under hot curing conditions. Furthermore, to reduce the cost, the alkaline to precursor ratio was reduced from 0.18 to 0.12, and mixture was pressed at 20 MPa molding pressure and more than 16 MPa strength was attained at ambient condition. It can be easily concluded that the observed compressive strength can be widely used in residential and commercial projects to fulfill the demand for construction materials and to reduce cement consumption.

Keywords: ambient cure; compressive strength; curing regimes; geopolymer mortar; hot curing; lime; molding pressure.

Introduction

Ordinary Portland Cement (OPC) is well renowned binding material but is considered an environmental burden due to a lot of CO_2 emissions. Several trials have been made by reducing the amount of cement in concrete by adding supplementary cementitious materials [1]. However, geopolymer materials are considered as the alternative material to cement paste, mortar, and concrete. Therefore, needs to be explored in more detail to replace conventional mortar or fired clay brick.

Geopolymers, which are considered part of alkali-activated materials, are one of the most promising materials in this respect. The process of geopolymerization involves the activation of rich silica and alumina materials in an alkaline environment [2]. The aluminosilicates are known as precursors such as clays (illite, halloysite, kaolinite, etc.) [3], and ashes (FA, bagasse ash, and rice husk ash, etc.) [4]. FA is a silica and alumina-rich precursor that is widely available in many countries. It has been used in cementitious products widely, many standards have also been developed for its efficient utilization [5]. The utilization of FA is only possible when it gets activated in an alkaline environment. In terms of the selection of a precursor, the basic philosophy to be kept in mind for obtaining a superior product is the degree of reaction based on the availability of amorphous

silica and alumina in the source material. Similarly, other parameters that influence the compressive strength during geopolymerization include alkaline to precursor and sodium silicate (Na_2SiO_3) to sodium hydroxide (NaOH) ratios, the molarity of NaOH and curing temperature, etc [6-8]. The mixture of NaOH and Na_2SiO_3 results in better strength development as compared to using them individually as an alkaline activator. Reducing the alkaline/precursor (A/P) ratio for FA-based geopolymer mortar decreases its cost. Another significant factor to consider, especially for geopolymerization, is the molding pressure [9-12], which might have a favorable impact on compressive strength. Pressure increases the rate of geopolymerization, but it also decreases porosity while increasing the bulk density. Moreover, there is a big variation in the temperature or curing condition of cement mortar as it requires very high temperature. Slag has been used along with the FA to cure the resultant geopolymer product at ambient conditions. Slag is rich in Calcium, and activated at the ambient condition to form the calcium-alumino-silicate-hydrate (C-A-S-H) gel and thus gets the strength [7]

With this background, a new couple has been proposed in this work, where FA was coupled with the LSP. Three curing regimes have been adopted to cure the specimen at ambient conditions and compare it concerning the hot curing condition. Hence, a systematic approach has been proposed in this work to synthesize geopolymer which fulfilled the mechanical strength criterion of ASTM standards for brick masonry.

Research Significance

OPC is used globally every year, and it contributes greatly to the world's CO_2 emissions. However, its use in concrete and mortar is environmentally unsustainable. This work was designed to develop FA-based geopolymer coupled with lime, a widely available material. The LSP was used without calcination to produce a cleaner environment. Moreover, the curing condition may also be the ambient or sun-dried condition to make it more sustainable. Hence, a systematic approach has been proposed in this work to synthesize geopolymer and to replace conventional concrete blocks or fired clay bricks. The authors believe that this study will have a positive effect on the construction industry.

Experimental Investigation

Materials

For the production of geopolymer mortar, FA, sand (river, dune), alkaline activators (NaOH, and Na_2SiO_3), LSP (calcium carbonate), and distilled water were used. The FA was classified as class F and having low calcium content (4.81%), because the total amount of SiO_2 (54.14%), Al_2O_3 (28.19), and Fe_2O_3 (4.93%) is higher than 70%, and the CaO content less than 10%, according to ASTM C 618 [13]. The color of FA was light grey having a density of 1058.6kg/m^3 . Types of sand used are River Sand (RS) and Dune Sand (DS). The sodium hydroxide (NaOH) was taken in pallet form having a white color. Sodium hydroxide was used to activate the FA so that FA exhibits good cementitious properties. Sodium Silicate was colorless and clear in physical properties. It was taken in gel form and also used to activate the FA. LSP was taken in powdered form and white color.

Specimens

Dry mixing of precursors i.e. FA and lime and filler material i.e. sand (river or dune) was carried out for 30 seconds with high speed mixer. By the addition of an alkaline activator, sodium silicate (Na_2SiO_3), and sodium hydroxide solution (NaOH), wet mixing was carried out for a further two min 30s, and a paste was formed. The work was divided into three series. In Series I, the paste was formed with 0.18 Alkaline/Precursor ratio (A/P) and 1.5 NaOH/ Na_2SiO_3 with the river sand and was filled in three layers in cube molds which were tested after placing under three curing regimes i.e. Oven-dry, Sun-dry, ambient dry. Then, the mix proportion was changed in Series II by reducing A/P to 0.12 and NaOH/ Na_2SiO_3 to 1.0, and cylinders (diameter of 71 mm) were filled with this paste in three layers with 12 times tamping at each layer. Then these were placed in the Universal Testing Machine (UTM) and a load was applied to obtain 20 MPa molding pressure. The specimen was taken out carefully from the cylindrical mold and was kept under ambient temperature. The same mix proportion was used in Series III with dune sand but it formed a slurry because of the change in porosity and surface roughness of particles so cubes of 2.75 mm in size were cast. A schematic diagram for preparation of geopolymer mortar specimens is shown in Fig. 1-1 and mix proportions for different series can be found in Table 1-1.

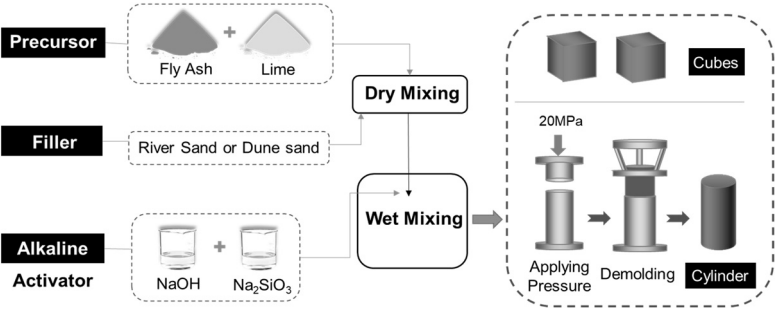


Fig. 1-1: Schematic Diagram of Specimen Preparation

Table 1-1: Summary of mix proportion and the specimens prepared in all series

Series	FA	Lime	Sand	$\text{Na}_2\text{SiO}_3/\text{NaOH}$	A/P	Pressure MPa	Curing
Series-I	40	10	50	1.50	0.18	N.A	Oven-Dry Sun-Dry Ambient
Series-II	40	10	50	1.0	0.18	20	Ambient
Series-III	40	10	50	1.0	0.18	N.A	Ambient